Coronal expansion and solar wind

- The solar corona over the solar cycle
- Coronal and interplanetary temperatures
- Coronal expansion and solar wind acceleration
- Origin of solar wind in magnetic network
- Multi-fluid modelling of the solar wind
- The heliosphere

Corona of the active sun

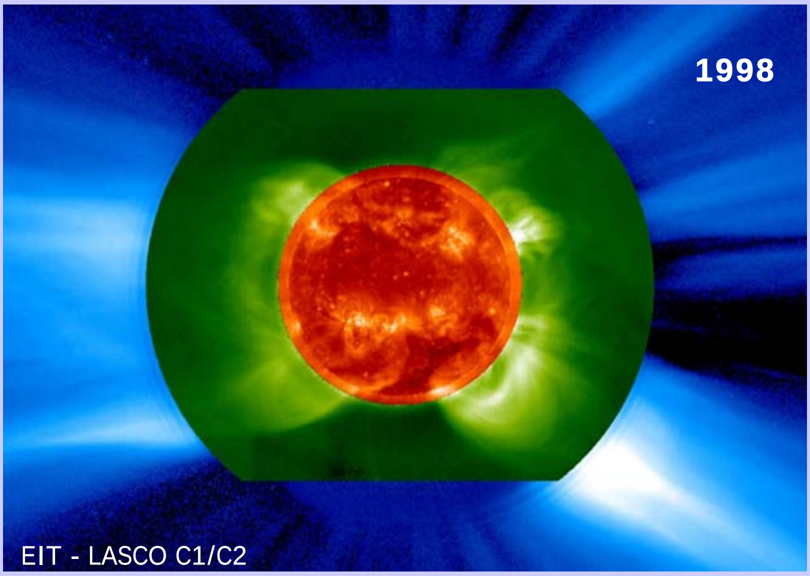

Solar wind speed and density

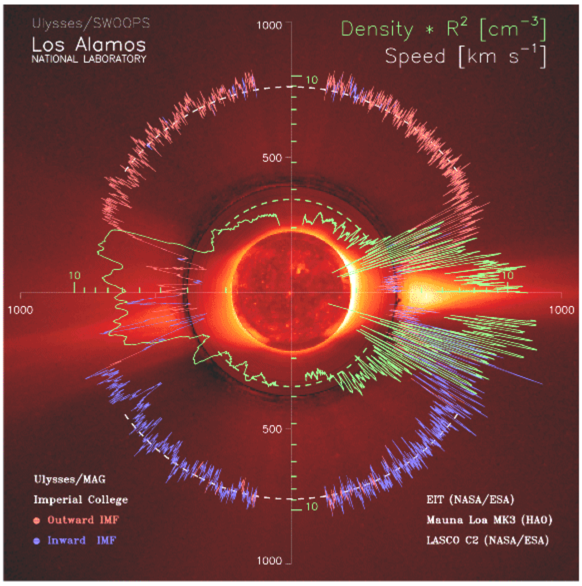

B outward

Ecliptic

B inward

McComas et al., GRL, **25**, 1, 1998

Polar diagram

V

Density

n R^2

Structure of the heliosphere

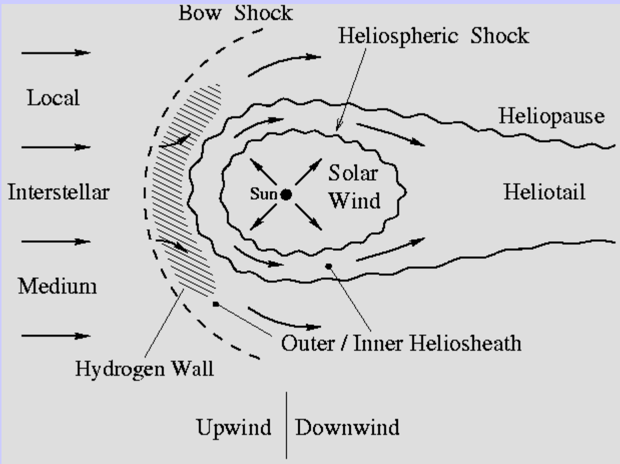

- Basic plasma motions in the restframe of the Sun
- Principal surfaces (wavy lines indicate disturbances)

Heliosphere and local interstellar medium

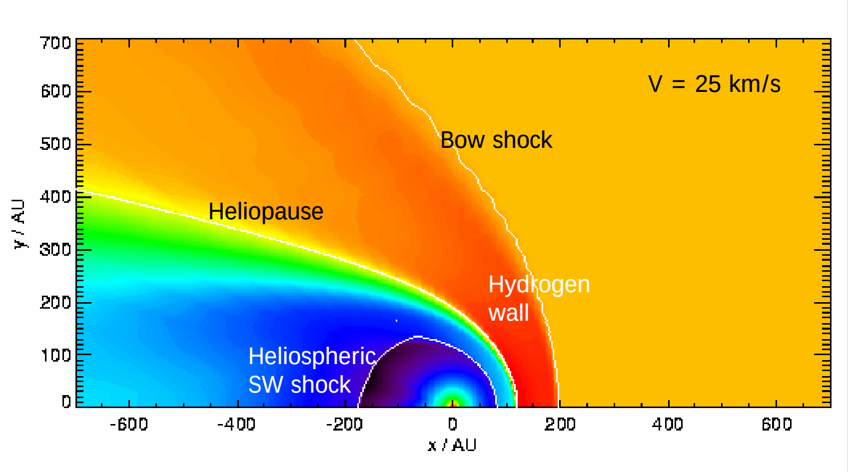

(red) - 0.3 > $\log(n_e/cm^3)$ > - 3.7 (blue)

Kausch, 1998

Energetics of the fast solar wind

- Energy flux at 1 R_S: F_E = 5 10^5 erg cm^{-2} s^{-1}
- Speed beyond 10 R_S: V_p = (700 - 800) km s^{-1}
- Temperatures at

  1.1 R_s: $T_e \approx T_p \approx$ 1-2 10^6 K

  1 AU: T_p = 3 10^5 K ; $T_\alpha = 10^6$ K ; T_e = 1.5 10^5 K
- Heavy ions: $T_i \cong m_i / m_p \, T_p$; $V_i - V_p = V_A$

$$\gamma/(\gamma-1)\, 2k_B T_S = 1/2 m_p (V_\infty^{\,2} + V^2)$$

γ=5/3, V_∞=618 kms^{-1}, $T_S = 10^7$ K for V_p=700 kms^{-1} --> 5 keV

Heliospheric magnetic field

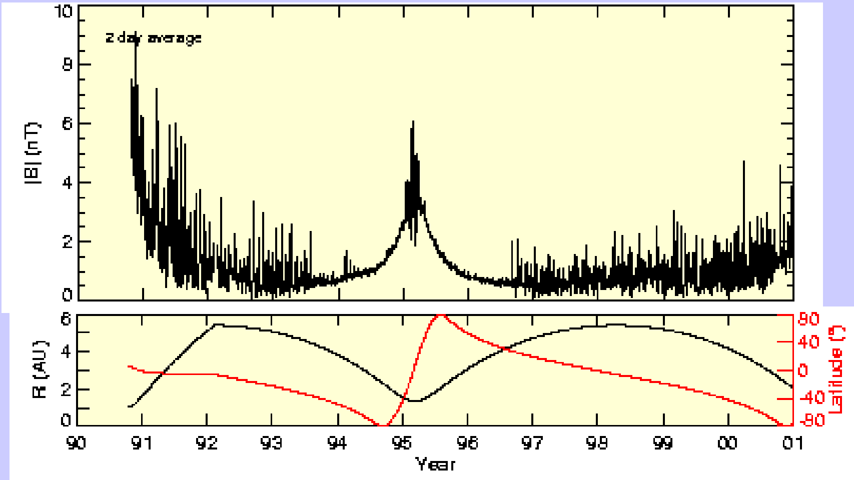

McComas et al., 1998

Ulysses SWOOPS

Changing corona and solar wind

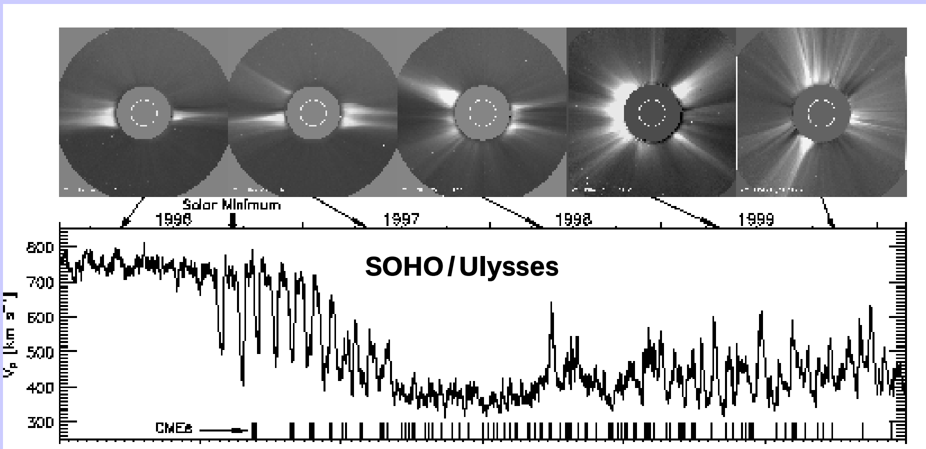

45 30 15 0 -15 -30 -45

North **Heliolatitude / degree** **South**

McComas et al., 2000

Evolution of the current sheet

Stack plot of Carrington rotations from 1983 to 1994, showing the location of the heliospheric current sheet (HCS) on the source surface at 2.5 R_s

Negative polarity, dark
Neutral line, bold

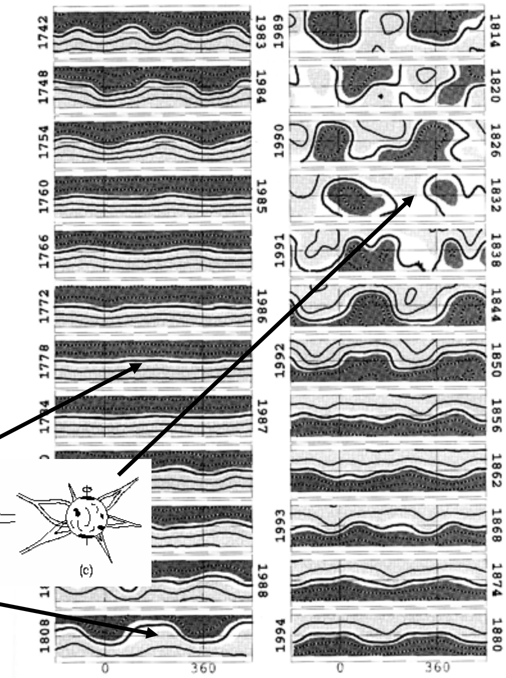

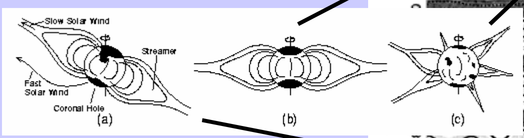

Hoeksema, Space Sci. Rev. **72**, 137, 1995

In situ current sheet crossings

Dense

Slow

Cold

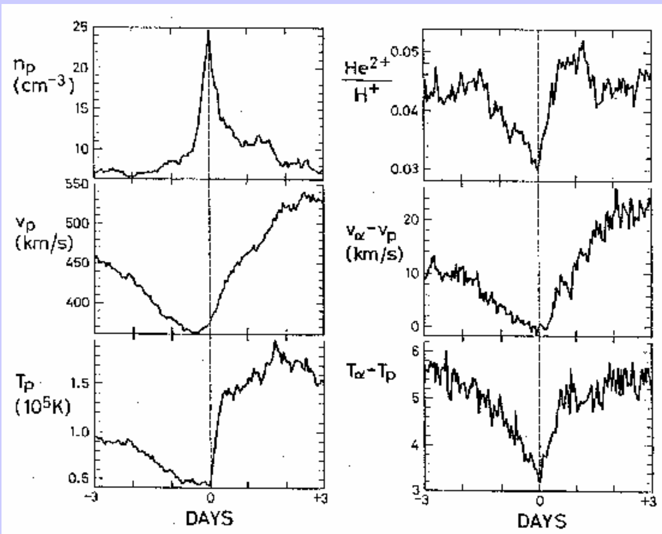

Less Helium

Speeds equal

Temperatures close

Borrini et al., JGR, 1981

Solar wind stream structure and heliospheric current sheet

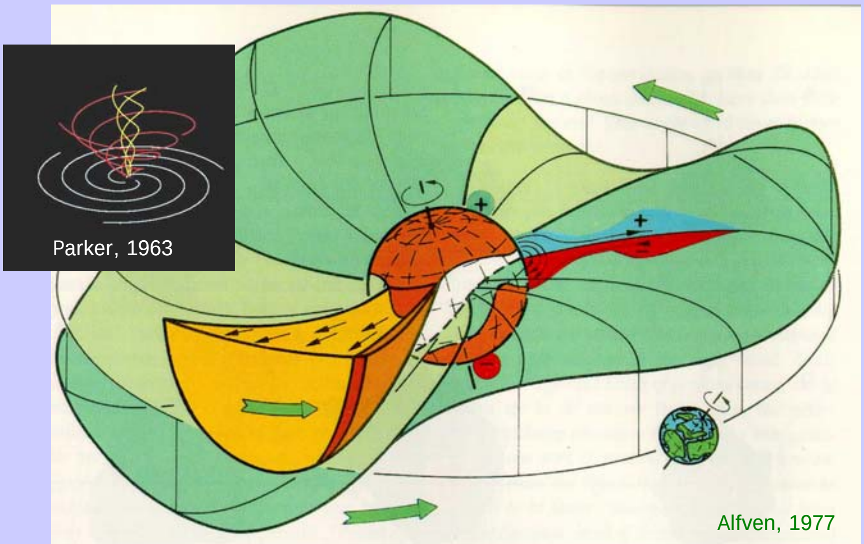

Solar wind fast and slow streams

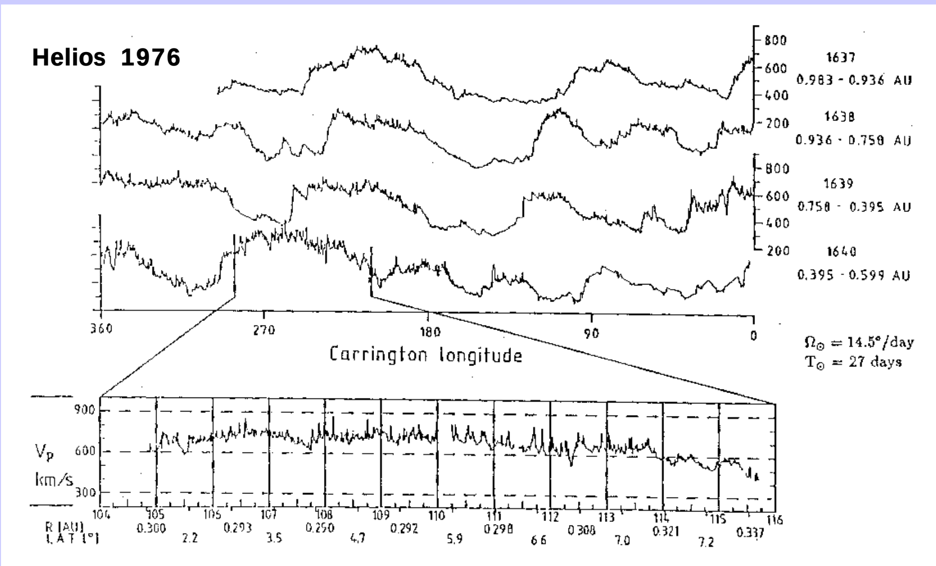

Alfvén waves and small-scale structures

Marsch, 1991

Solar wind data from Ulysses

V

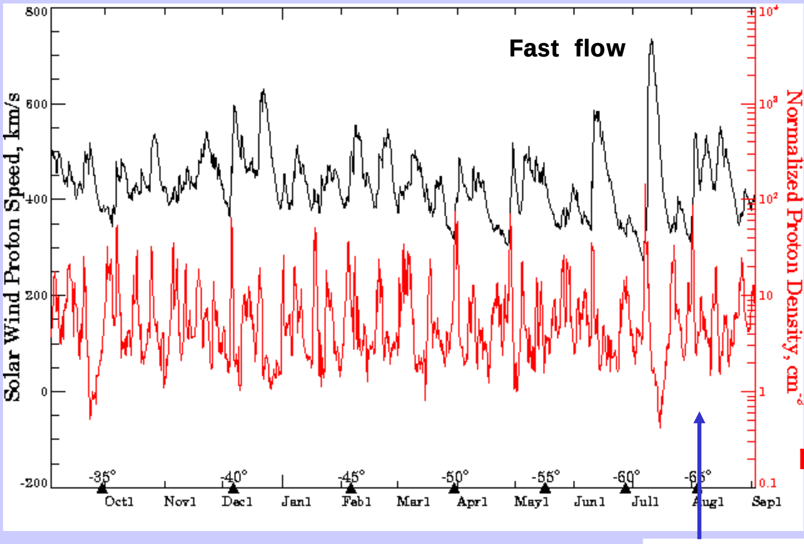

n

McComas et al., 2000 **September 3, 1999 - September 2, 2000** **Latitude: - 65°**

Solar wind types

1. Fast wind near activity minimum

High speed	400 - 800 kms^{-1}
Low density	3 cm^{-3}
Low particle flux	2 x 10^{8} cm^{-2} s^{-1}
Helium content	3.6%, stationary
Source	coronal holes
Signatures	stationary for long times (weeks!)

2. Slow wind near activity minimum

Low speed	250 - 400 km s^{-1}
High density	10 cm^{-3}
High particle flux	3.7 x 10^{8} cm^{-2} s^{-1}
Helium content	below 2%, highly variable
Source	helmet streamers near current sheet
Signatures	sector boundaries embedded

Schwenn, 1990

Solar wind types

3. Slow wind near activity maximum

Similar characteristics as 2., except for

Helium content	4%, highly variable
Source	active regions and small CHs
Signatures	shock waves, often imbedded

4. Solar ejecta (CMEs), often associated with shocks

High speed	400 - 2000 kms^{-1}
Helium content	high, up to 30%
Other heavy ions	often Fe^{16+} ions, in rare cases He^{+}
Signatures	often magnetic clouds, about 30% of the cases related with erupting prominences

Schwenn, 1990

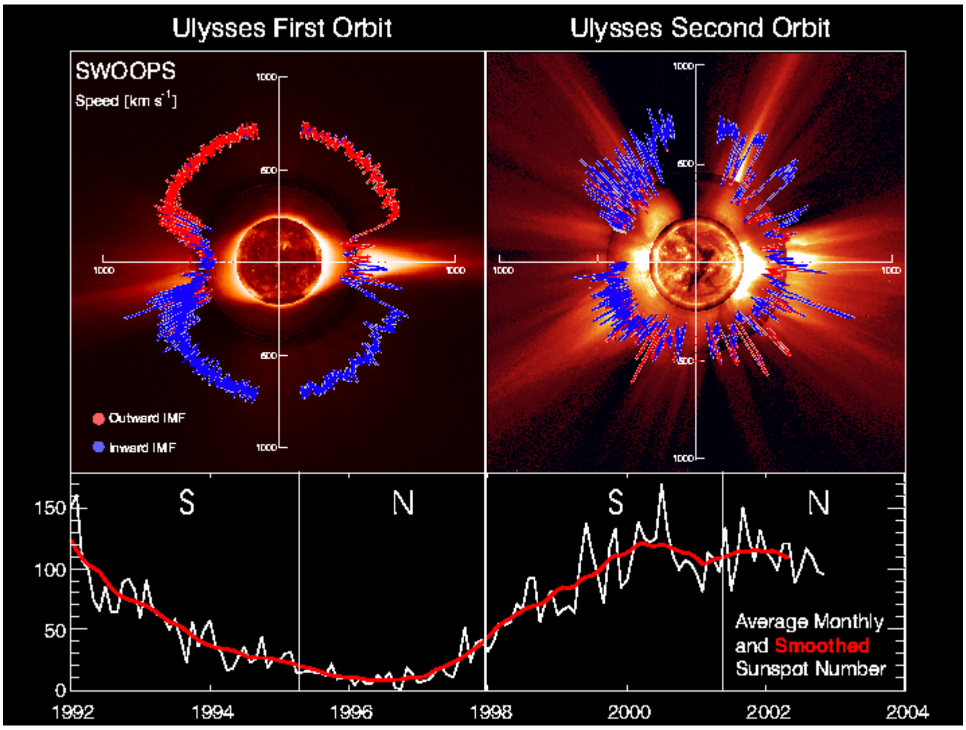

Heliospheric temperatures

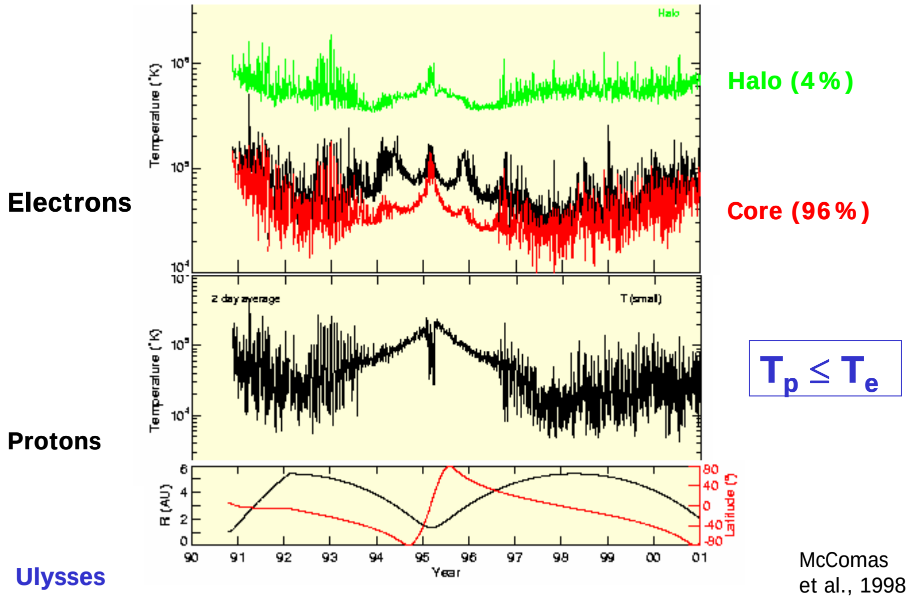

$T_p \leq T_e$

McComas et al., 1998

Fast solar wind speed profile

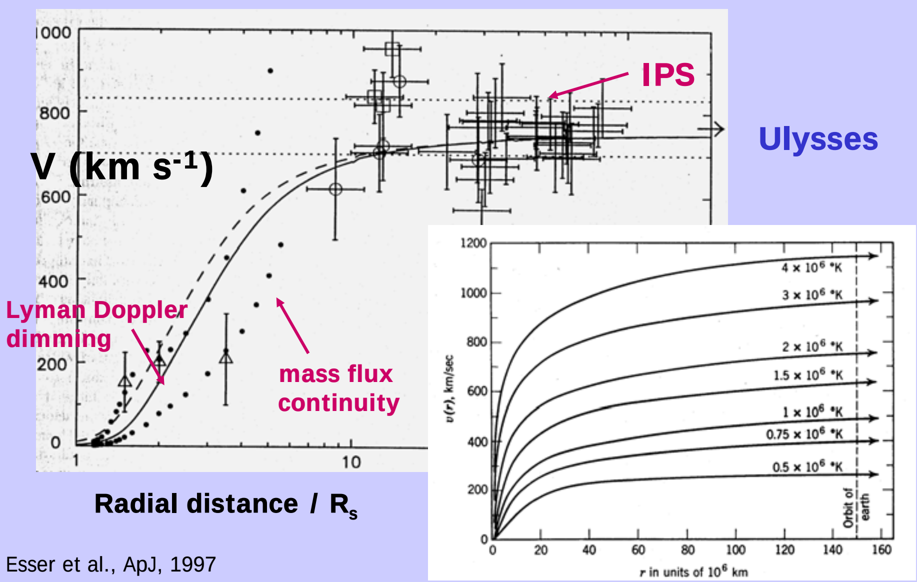

Esser et al., ApJ, 1997

Speed profile of the slow solar wind

Speed profile as determined from plasma blobs in the wind

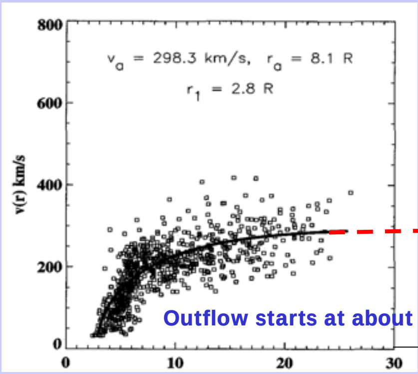

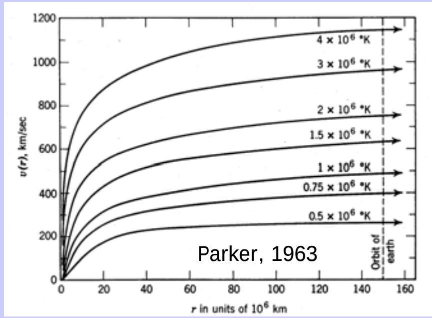

Outflow starts at about 3 R_S

Radial distance / R_S 60

Sheeley et al., Ap.J., **484**, 472, 1998

Consistent with Helios data

Solar wind models I

Assume heat flux, $Q_e = -\rho\kappa\nabla T_e$, is free of divergence and thermal equilibrium: $T = T_p = T_e$. Heat conduction: $\kappa = \kappa_o T^{5/2}$ and $\kappa_o = 8\ 10^8$ erg/(cm s K); with $T(\infty) = 0$ and $T(0) = 10^6$K and for spherical symmetry:

$$4\pi r^2 \kappa(T) dT/dr = \text{const} \quad \text{-->} \quad T = T_0 (R/r)^{2/7}$$

Density: $\rho = n_p m_p + n_e m_e$, quasi-neutrality: $n = n_p = n_e$, thermal pressure: $p = n_p k_B T_p + n_e k_B T_e$, then with hydrostatic equilibrium and $p(0) = p_0$:

$$dp/dr = -GMm_p n/r^2$$

$$\boxed{p = p_0 \exp[\,(7GMm_p)/(5k_B T_0 R)\ (\ (R/r)^{5/7} - 1)\ ]}$$

Problem: $p(\infty) > 0$, therefore corona must expand!

Chapman, 1957

Solar wind models II

Density: $\rho = n_p m_p + n_e m_e$, quasi-neutrality: $n = n_p = n_e$, ideal-gas thermal pressure: $p = n_p k_B T_p + n_e k_B T_e$, thermal equilibrium: $T = T_p = T_e$, then with hydrodynamic equilibrium:

$$mn_p V\, dV/dr = - dp/dr - GMm_p n/r^2$$

Mass continuity equation:

$$mn_p V r^2 = J$$

Assume an isothermal corona, with sound speed $c_0 = (k_B T_0/m_p)^{1/2}$, then one has to integrate the DE:

$$\boxed{[(V/c_0)^2 - 1]\, dV/V = 2\,(1 - r_c/r)\, dr/r}$$

With the critical radius, $r_c = GMm_p/(2k_B T_0) = (V_\infty/2c_0)^2$, and the escape speed, V_∞ = 618 km/s, from the Sun's surface.

Parker, 1958

Solar wind models III

Introduce the sonic Mach number as, $M_s = V/c_0$, then the integral of the DE (C is an integration constant) reads:

$$(M_s)^2 - \ln(M_s)^2 = 4\,(\ln(r/r_c) + r_c/r) + C$$

For large distances, $M_s >> 1$; and $V \sim (\ln r)^{1/2}$, and $n \sim r^{-2}/V$, reflecting spherical symmetry.

Only the „wind" solution IV, with C=-3, goes through the critical point r_c and yields: n -> 0 and thus p -> 0 for r -> ∞. This is Parker's famous solution: the solar wind.

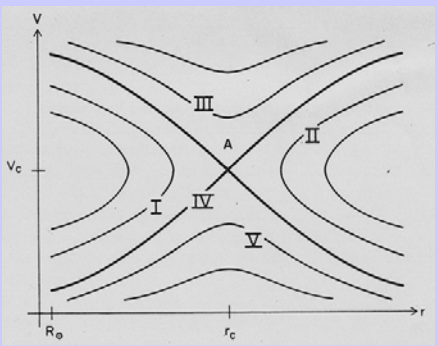

Parker, 1958

V, solar breeze; III accretion flow

On the source regions of the fast solar wind in coronal holes

Image: EIT
Corona in
Fe XII 195 Å
at 1.5 M K

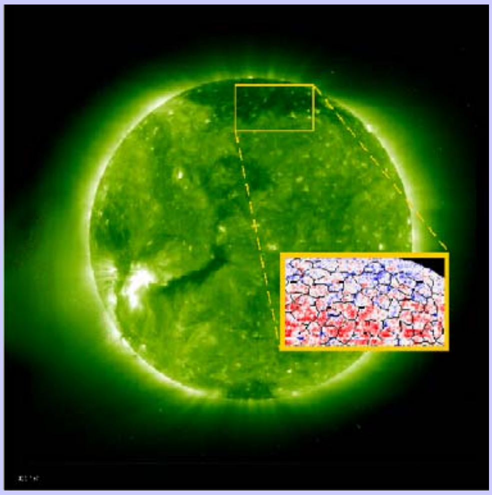

Insert: SUMER
Ne VIII 770 Å
at 630 000 K

Chromospheric network
Doppler shifts
Red: down
Blue: up

Outflow at lanes and junctions

Hassler et al.,
Science 283,
811-813, 1999

Polar coronal hole

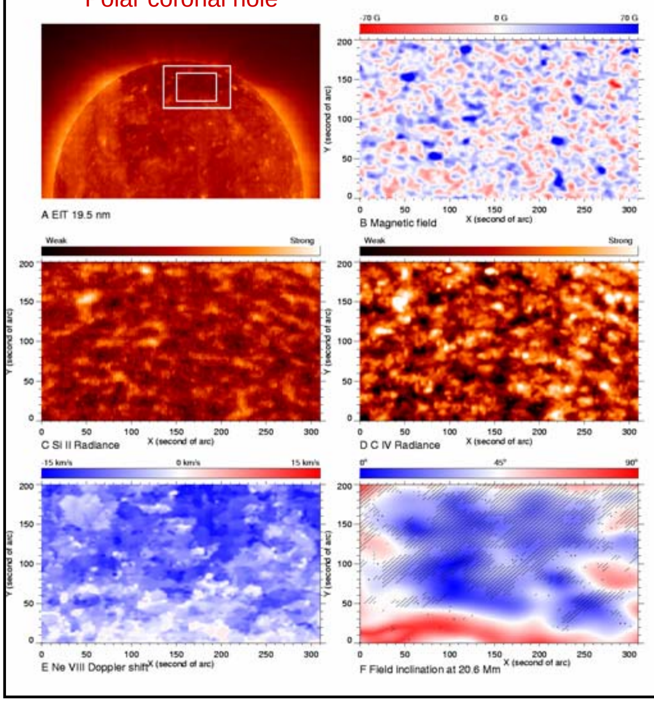

Outflow

(A) Sun in EIT wavelength window around 19.5 nm. The white rectangle indicates the size of the SUMER raster scan. A comparison of the structures was made only for the smaller rectangle.
(B) Magnetic field vertical component from –70 to 70 G
(C) Si II radiance in arbitrary units (chromosphere)
(D) C IV radiance in arbitrary units (transition region)
(E) Ne VIII Doppler shifts along the LOS, ranging from –15 km/s to 15 km/s.
(F) Comparison between the Ne VIII Doppler shift (hatched regions with outflow speeds higher than 7 km/s) and the magnetic field angle, with 0° indicating vertical and 90° horizontal orientation at a height of 20.6 Mm.

Tu et al., Science 2005

Loops and funnels in equatorial CH

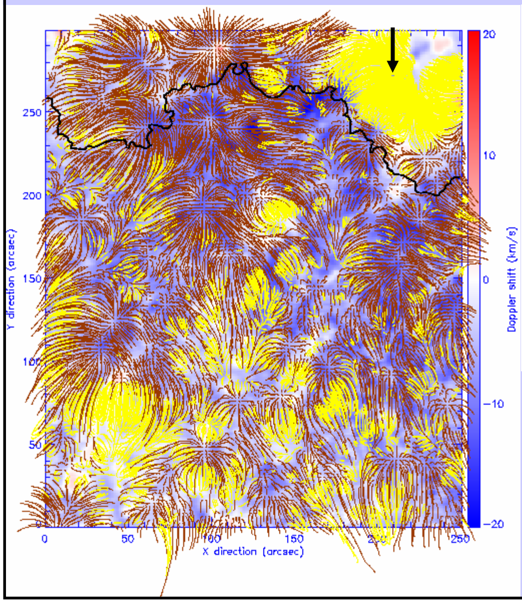

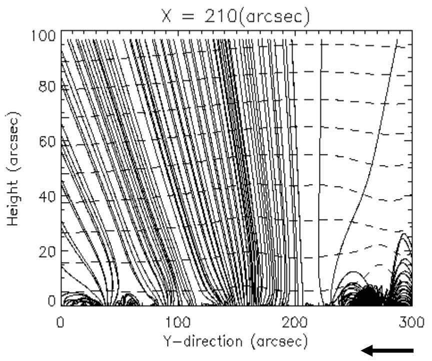

Field lines: brown open, and yellow closed

Correlation: Field topology and plasma outflow (blue in open field)

Wiegelmann, Xia, and Marsch, A&A, 432, L1, 2005

Height profiles in funnel flows

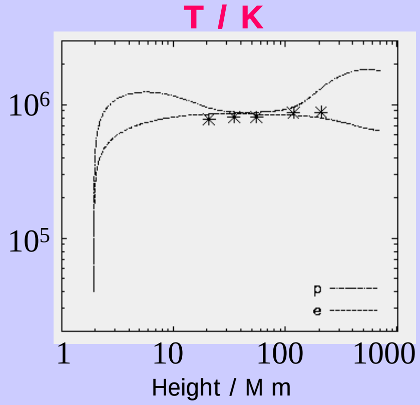

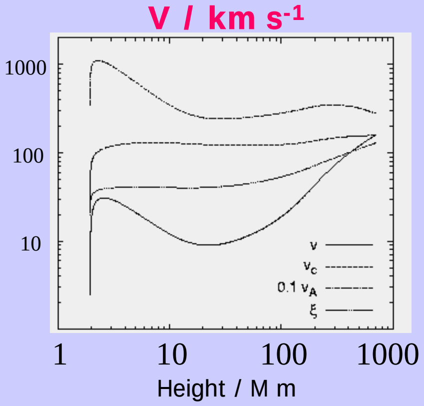

- Critical point at 1 R_S

- Heating by wave sweeping
- Steep temperature gradients

Hackenberg, Marsch, Mann, A&A, **360**, 1139, 2000

Flows and funnels in coronal hole

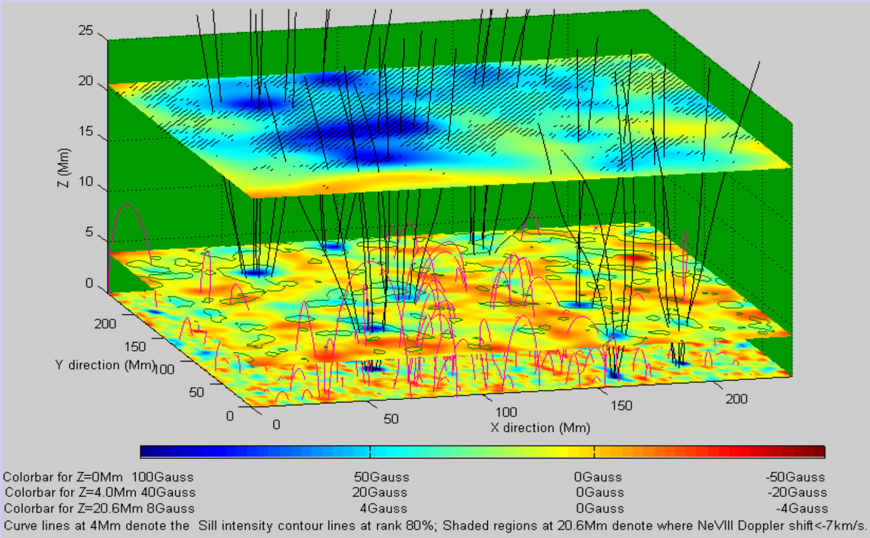

Tu, Zhou, Marsch, et al., Science, 308, 519, 2005

Mass and energy supply

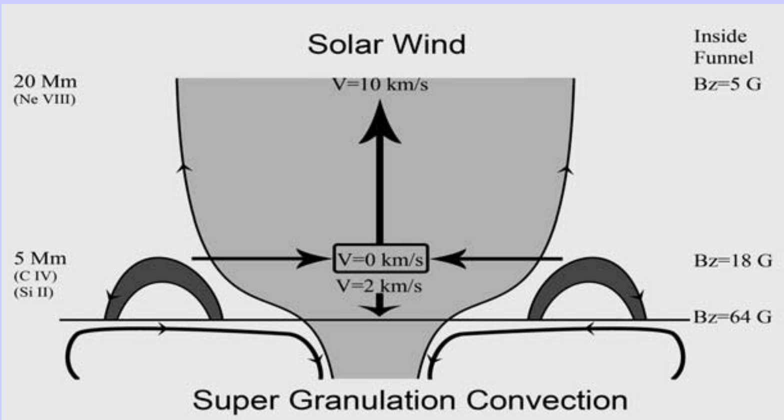

Sketch to illustrate the scenario of the solar wind origin and mass supply. The plot is drawn to show that supergranular convection is the driver of solar wind outflow in coronal funnels. The sizes and shapes of funnels and loops shown are drawn according to the real scale sizes of the magnetic structures.

Detailed source region

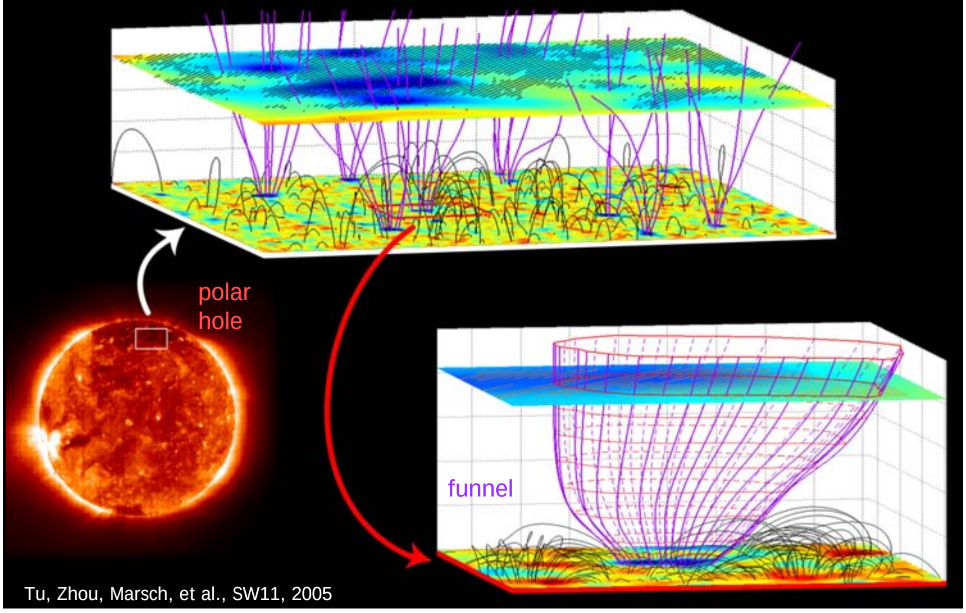

Tu, Zhou, Marsch, et al., SW11, 2005

Rotation of the sun and corona

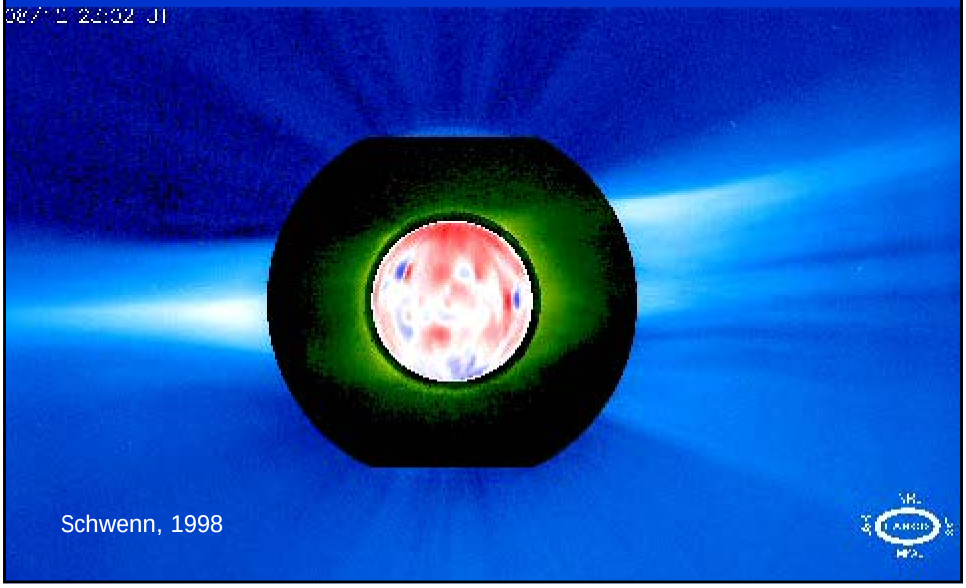

Schwenn, 1998

Rotation of solar corona

Fe XIV

5303 Å

Time series:

1 image/day

(24-hour

averages)

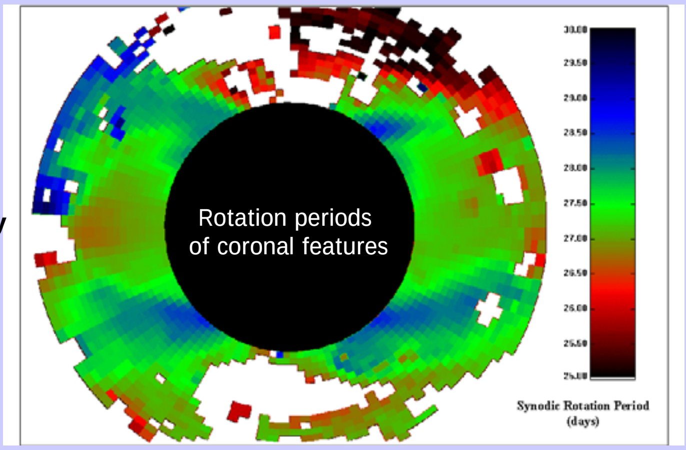

27.2
days

LASCO
/SOHO

Stenborg et al., 1999

Long-lived coronal patterns exhibit uniform rotation at the equatorial rotation period!

Sun's loss of angular momentum carried by the solar wind

Induction equation:

$\nabla \times (\mathbf{V} \times \mathbf{B}) = 0$ **-->** $r\,(V_r B_\phi - B_r V_\phi) = -\,r_0 B_0 \Omega_0 r_0$

Momentum equation:

$\rho \mathbf{V} \bullet \nabla V_\phi = 1/4\pi\, \mathbf{B} \bullet \nabla B_\phi$ **-->** $r\,(\rho\, V_r V_\phi - B_r B_\phi) = 0$

$\mathbf{L = \Omega_0 r_A^2}$ (specific angular momentum)

$V_\phi = \Omega_0 r\,(M_A^2\,(r_A/r)^2 - 1)/(M_A^2 - 1)$

$M_A = V_r (4\pi\rho)^{1/2}/B_r$

Alfvén Machnumber

Weber & Davis, ApJ, **148**, 217, 1967

Helios: $r_A = 10\text{-}20\ R_s$

(Parker) spiral interplanetary magnetic field

rot(**E**) = rot(**V**X**B**) = **0**

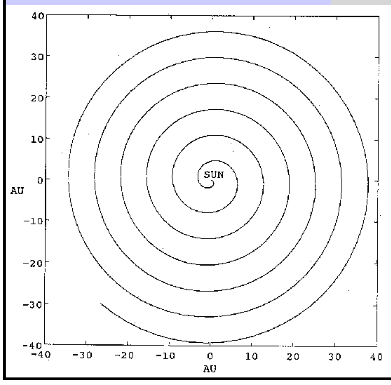

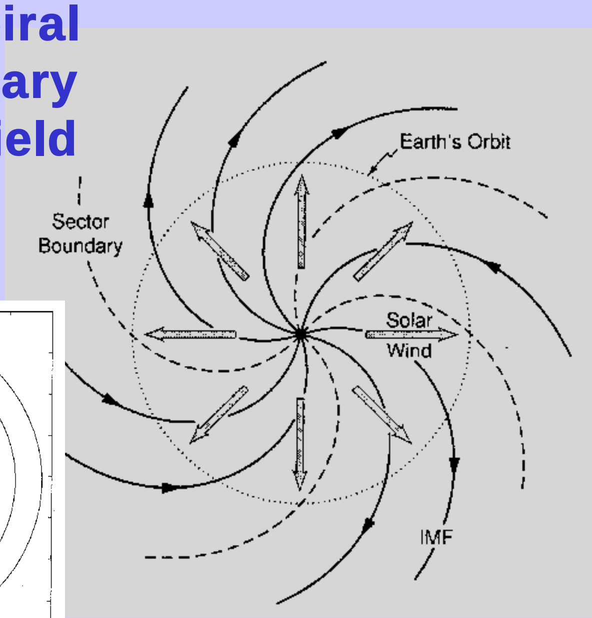

Fluid equations

- **Mass flux:** $F_M = \rho V A$ $\rho = n_p m_p + n_i m_i$
- **Magnetic flux:** $F_B = B A$
- **Total momentum equation:**

$$\boxed{V\, d/dr\, V = -1/\rho\, d/dr\,(p + p_w) - GM_S/r^2 + a_w}$$

- **Thermal pressure:** $p = n_p k_B T_p + n_e k_B T_e + n_i k_B T_i$
- **MHD wave pressure:** $p_w = (\delta B)^2/(8\pi)$
- **Kinetic wave acceleration:** $a_w = (\rho_p a_p + \rho_i a_i)/\rho$
- **Stream/flux-tube cross section:** $A(r)$

Model of the fast solar wind

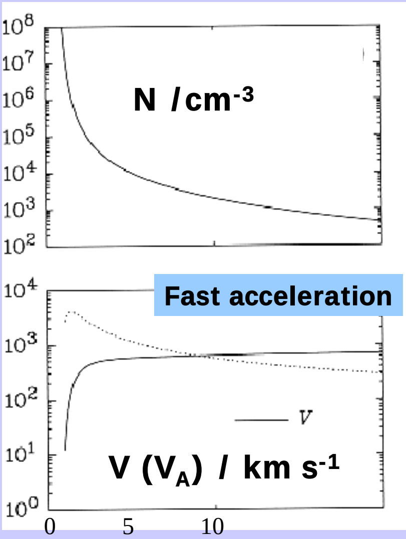

Radial distance / R_S

Low density, $n \approx 10^8$ cm^{-3}, consistent with coronagraph measurements

T / K

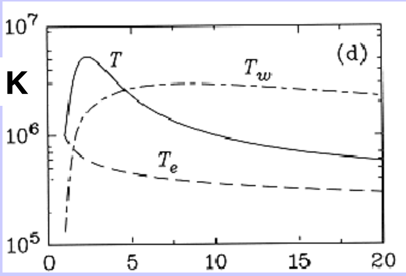

- **hot protons, $T_{max} \approx 5$ M K**
- **cold electrons**
- **small wave temperature, T_w**

McKenzie et al., Geophys. Res. Lett., **24**, 2877, 1997

The future: Solar Orbiter

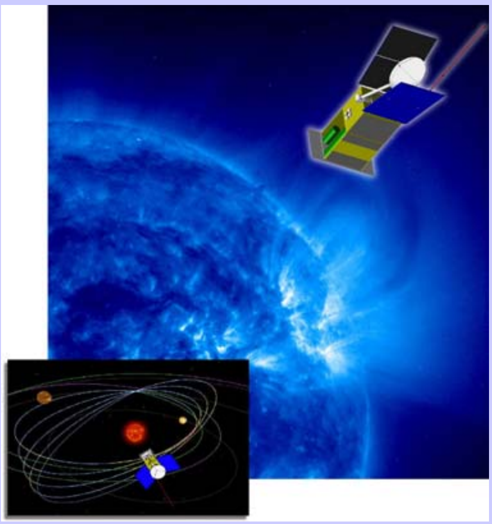

A high-resolution mission to the Sun and inner heliosphere

ESA

2015